

Video Article

# Ratiometric Imaging of Extracellular pH in Dental Biofilms

Sebastian Schlafer<sup>1</sup>, Irene Dige<sup>1</sup>

<sup>1</sup>Department of Dentistry, Aarhus University

Correspondence to: Sebastian Schlafer at [sebastians@microbiology.au.dk](mailto:sebastians@microbiology.au.dk)

URL: <https://www.jove.com/video/53622>

DOI: [doi:10.3791/53622](https://doi.org/10.3791/53622)

Keywords: Immunology, Issue 109, Biofilm, confocal microscopy, dental caries, extracellular pH, pH ratiometry, ratiometric dye

Date Published: 3/9/2016

Citation: Schlafer, S., Dige, I. Ratiometric Imaging of Extracellular pH in Dental Biofilms. *J. Vis. Exp.* (109), e53622, doi:10.3791/53622 (2016).

## Abstract

The pH in bacterial biofilms on teeth is of central importance for dental caries, a disease with a high worldwide prevalence. Nutrients and metabolites are not distributed evenly in dental biofilms. A complex interplay of sorption to and reaction with organic matter in the biofilm reduces the diffusion paths of solutes and creates steep gradients of reactive molecules, including organic acids, across the biofilm. Quantitative fluorescent microscopic methods, such as fluorescence life time imaging or pH ratiometry, can be employed to visualize pH in different microenvironments of dental biofilms. pH ratiometry exploits a pH-dependent shift in the fluorescent emission of pH-sensitive dyes. Calculation of the emission ratio at two different wavelengths allows determining local pH in microscopic images, irrespective of the concentration of the dye. Contrary to microelectrodes the technique allows monitoring both vertical and horizontal pH gradients in real-time without mechanically disturbing the biofilm. However, care must be taken to differentiate accurately between extra- and intracellular compartments of the biofilm. Here, the ratiometric dye, semaphthorhodafuor-4F 5-(and-6) carboxylic acid (C-SNARF-4) is employed to monitor extracellular pH in *in vivo* grown dental biofilms of unknown species composition. Upon exposure to glucose the dye is up-concentrated inside all bacterial cells in the biofilms; it is thus used both as a universal bacterial stain and as a marker of extracellular pH. After confocal microscopic image acquisition, the bacterial biomass is removed from all pictures using digital image analysis software, which permits to exclusively calculate extracellular pH. pH ratiometry with the ratiometric dye is well-suited to study extracellular pH in thin biofilms of up to 75  $\mu$ m thickness, but is limited to the pH range between 4.5 and 7.0.

## Video Link

The video component of this article can be found at <https://www.jove.com/video/53622/>

## Introduction

The method described here allows monitoring extracellular pH in dental biofilms in the range between 4.5 and 7, using the ratiometric dye semaphthorhodafuor-4F 5-(and-6) carboxylic acid (C-SNARF-4) in combination with confocal laser scanning microscopy and digital image analysis. The employed fluorescent dye is pH-sensitive and displays a shift in its fluorescent emission depending on the state of protonation. The fluorescent emission of the protonated molecule peaks at 580 nm, and the emission of the deprotonated molecule at 640 nm<sup>1</sup>. The ratio of the fluorescent emission intensities in two detection windows comprising the two emission peaks (576 - 608 nm and 629 - 661 nm) thus reflects pH in the liquid phase, irrespective of dye concentration. With a pK<sub>a</sub> of ~6.4 the dye is suitable to visualize pH in moderately acidic environments.

pH in bacterial biofilms is of central importance for all metabolic processes. In the case of dental biofilms, pH in the extracellular matrix is the key virulence factor for the development of dental caries. Extended periods with low pH at the biofilm-tooth interface lead to slow demineralization of the underlying enamel<sup>2</sup>. Due to the complex three-dimensional architecture of biofilms, metabolites, including organic acids, are not uniformly distributed across the biofilm. Highly and less acidogenic microenvironments may be found in close spatial proximity<sup>3</sup>.

For decades, vertical pH gradients in biofilms were recorded with the help of microelectrodes<sup>4-6</sup>. While they offer a good spatial resolution due to their small tip size, they are not well-suited to monitor horizontal gradients. Moreover, insertion of the electrode disturbs the biofilm mechanically. Quantitative fluorescent microscopic techniques offer the advantage of visualizing pH changes in different areas of a biofilm without mechanical interference. Different microscopic fields of view can be selected freely and imaged repeatedly over prolonged periods<sup>1,7-9</sup>. However, when interpreting microscopic biofilm images, it is important to distinguish between fluorescence deriving from the microbial biomass and fluorescence deriving from the extracellular space. In acidic conditions, pH inside bacterial cells is different from pH in the extracellular matrix, as the bacteria actively transport protons across their cell membrane at the expense of adenosine triphosphate<sup>10</sup>. In the context of dental caries, intracellular bacterial pH does not have a direct impact on the underlying enamel whereas low extracellular pH leads to demineralization. Averaging pH in microscopic images that contain both bacteria-free areas and bacteria leads to erroneous results. The use of other stains along with the pH-sensitive dye in order to visualize the bacterial biomass and differentiate between extra- and intracellular areas brings about the risk of fluorescent contamination of the extracellular space and false measurements<sup>11</sup>.

The present manuscript therefore describes the use of the ratiometric dye in a double function; both as a pH marker and as a universal bacterial stain. As the dye is up-concentrated in bacterial cells, the combination of confocal microscopic imaging and an accurate digital image analysis procedure allows determining extracellular pH in the range between 4.5 and 7.0 in thin dental biofilms.

## Protocol

The experimental protocol was reviewed and approved by the Ethics Committee of Aarhus County (M-20100032).

### 1. Confocal Microscopic Calibration of the Ratiometric Dye

- For image acquisition, use an inverted confocal microscope equipped with an incubator, a 63X/1.2-numeric aperture water immersion objective, a 543 nm laser line and a META detector.
- Prepare HEPES buffer stock solutions (50 mM, adjusted to pH 4.5-8.5 in steps of 0.1 pH units). Pipette 100  $\mu$ l of each solution into the wells of a clear-bottom 96-well plate for fluorescent microscopy.
- Wear nitrile gloves when handling the ratiometric dye C-SNARF-4. Prepare a 1 mM stock solution of the dye in dimethyl sulfoxide. Add 5  $\mu$ l of the stock solution to each well with HEPES buffer. Place the 96-well plate on the microscope.
- Turn on the microscope. Open the microscope software. Click the following panels: Acquire  $\rightarrow$  Laser; Acquire  $\rightarrow$  Micro; Acquire  $\rightarrow$  Config; Acquire  $\rightarrow$  Scan; Acquire  $\rightarrow$  Stage. Warm up the incubator to 37  $^{\circ}$ C.
- Turn on the 543 nm laser line by clicking on the 543 nm laser and the "On" button in the "Laser Control" window. Choose the 63X/1.2-numeric aperture water immersion objective in the "Microscope Control" window.
- Set the META detector to simultaneously monitor fluorescence within 576- to 608-nm (green) and 629- to 661 nm (red) intervals ("Configuration Control"  $\rightarrow$  "ChS"). Adjust the laser power ("Configuration Control"  $\rightarrow$  "Excitation"). Set the pinhole to yield an optical slice thickness of 1.6  $\mu$ m ("Scan Control"  $\rightarrow$  "Pinhole").
- Acquire an image of each HEPES buffer solution, 5  $\mu$ m above the glass bottom of the 96-well plate. Note: As soon as the focus plane is situated below the glass bottom, no fluorescent light can be seen on the screen. After every third image, set the laser power to zero and take an image for background subtraction.
- Perform the calibration experiment in triplicate (1.2-1.7).
- Determine the average fluorescent intensity and standard deviation in all red and green images.
  - Calculate the ratio  $R$  and standard error of mean,  $S_R$ , for each image according to equations (1) and (2)

$$(1) R = \frac{g - b_g}{r - b_r}$$

$$(2) S_R = \frac{1}{n \cdot (r - b_r)} \left( s_g^2 + s_{bg}^2 + R^2 \cdot (s_r^2 + s_{br}^2) \right)^{1/2}$$

$g$ ,  $r$ ,  $s_g$  and  $s_r$  are the averages and standard deviations in the respective green and red images.  $b_g$ ,  $b_r$ ,  $s_{bg}$  and  $s_{br}$  are the corresponding values for the background images.  $n^2$  is number of pixels imaged.

- Plot the calculated ratios for each pH value from the three replicate calibration experiments in a diagram and construct a fitted curve from this series of data points (*i.e.* using the software SigmaPlot 13). Make a mathematical function from the fitted curve that can convert ratios into pH values<sup>10</sup>.

### 2. Collection of *In Situ* Grown Dental Biofilm Samples

- Select volunteers that fulfill inclusion and exclusion criteria relevant for the study. Make alginate impressions of their upper and lower dental arch. Make cast models from these impressions and manufacture an acrylic splint in the lower jaw. Design the splint with buccal acrylic flanges connected by a lingual orthodontic wire that allows the volunteer to bite into normal occlusion<sup>12</sup>.
- Drill recessions in the buccal flanges of the acrylic splint (**Figure 1**) with the help of dental acrylic burs to allow insertion of glass slabs for biofilm collection. The depth of the recessions should be at least 1.5 mm, while the width and length of the recessions may vary depending on the number of glass slabs to be inserted.
- For biofilm collection, use custom-made non-fluorescent glass slabs (4 x 4 x 1 mm<sup>3</sup>) with a surface roughness of grit 1,200 in order to mimic the colonization pattern on natural enamel<sup>11</sup>.
- Sterilize the glass slabs by autoclaving prior to mounting. Mount the glass slabs with sticky wax in the depressions in the buccal flanges of each side slightly recessed to the surface of the acrylic surface in order to protect the biofilm from shear forces exerted by movement of the cheeks<sup>11</sup>.  
Note: The number of glass slabs placed in a recession may vary between 3 and 14, depending on the aim of the study.
- Insert the appliance in the mouth of the volunteer. Instruct the volunteer to retain the appliance intra-orally throughout the experimental period. Instruct the volunteer to store the appliance in an orthodontic retainer container with a piece of wet paper tissue (to keep it humid) at room temperature during tooth brushing and intake of food and beverages other than water. Instruct the volunteer to not touch the buccal acrylic flanges with the glass slabs while placing and removing the appliance.  
Note: The experimental period may vary depending on the aim of the study (one day to several weeks).
- Carefully remove the glass slabs from the appliance at the end of the experimental period. Remove the sticky wax around the slabs with a knife and transfer them with a pair of tweezers to a closed container, the biofilm facing upward, until microscopic analysis. Keep the container humid with wet paper tissue. Perform pH imaging within few hours after biofilm collection.

### 3. Biofilm pH Imaging

1. Prepare salivary solution by adding dithiothreitol to collected saliva according to the method of de Jong *et al.*<sup>13</sup>. Titrate the salivary solution to pH 7.0 and add glucose to a concentration of 0.4 % (wt/vol). Pipette 100  $\mu$ l per biofilm to be analyzed into a glass-bottom 96-well plate for microscopy. Add 5  $\mu$ l of the ratiometric dye per well.
2. Place the 96-well plate on the microscope stage. Turn on the microscope and the 543 nm laser line. Warm up the incubator to 37 °C. Use the same microscope settings as for the calibration of the dye (see steps 1.5-1.6). Wait for 30 min, until the 96-well plate has reached working temperature.
3. Pick up one or more glass slabs with a slim set of tweezers and place them in the saliva-filled wells, one slab per well, with the biofilms facing downward.
4. Acquire single images ("Scan Control" → "Single") or z-stacks ("Scan Control" → "Start") spanning the depth of the biofilms in different areas. To acquire z-stacks choose the number of slices to be imaged ("Scan Control" → "Z Settings" → "Num Slices") and mark the z-position for the first and the last slice in the microscope software ("Scan Control" → "Z Settings" → "Mark First"; "Mark Last").  
Note: Z-stacks with a depth of up to 75  $\mu$ m can be acquired with good contrast between extracellular and intracellular areas.
5. To follow pH changes in a microscopic field of view over time, mark the x-y-position in the microscope software ("Stage and Focus Control" → "Mark Pos") and take repeated images at consecutive time points ("Scan Control" → "Single"). Regularly take images with the laser power set to zero for background subtraction.

### 4. Digital Image Analysis

1. To export the microscopic images as TIF files, use the file batch export of the microscope software ("Macro" → "File Batch Export"). Mark the files to be exported and save red and green channel images in separate folders as TIF-files ("Start Batch Export"). Rename the files in both folders giving them sequential numbers.
2. Import the red and green image series into software such as daime (digital image analysis in microbial ecology)<sup>14</sup>. Segment the green channel images with individually chosen brightness thresholds (Segment → Automatic segmentation → Custom threshold). Choose the brightness thresholds with care (typically between 20 and 80), so that all bacteria (brighter than the extracellular matrix), but not the matrix will be recognized as objects during segmentation. Verify visually that the areas recognized as objects correspond well to the bacterial biomass.
3. Transfer the object layer of the segmented green channel images to the corresponding red channel images (Segment → Transfer object layer). Use the object editor function to reject and delete all objects in the red and green channel images. Now only the extracellular matrix is left in the biofilm images. Export the processed image series as TIF files.
4. Import the image series into ImageJ (<http://rsb.info.nih.gov/ij/>; v.1.47). Determine the average fluorescence intensity in the background images taken with the laser turned off (Analyze → Histogram). Subtract the appropriate background from the red and green images (Process → Math → Subtract).
5. Still in ImageJ, divide the green image series (G1) by itself (Process → Image calculator). Then multiply the resulting image series (G2) with the green image series (G1). This will yield an image series (G3), where NaN is assigned to all pixels belonging to areas that were recognized as objects in daime. Proceed in the same way with the red image series ( $R1/R1 = R2$ ;  $R2 \times R1 = R3$ ).  
Note: As the bacterial biomass was removed from the images in step 4.3, the fluorescent intensity is 0 in these areas. Step 4.5 is necessary to convert the value 0 to NaN, which allows for ratio calculation in step 4.6.
6. Apply the 'Mean' filter (Process → Filters → Mean; radius: 1 pixel) to compensate for detector noise. Divide the green image series by the red image series (Process → Image calculator). This results in a green/red ratio for every remaining pixel in the extracellular space of the images. Use false coloring for graphic representation of the ratios in the images (Image → Lookup Tables). Calculate the mean ratio for each image (Analyze → Histogram).
7. Convert the green/red ratios to pH values according to the function fitted under 1.9.2). Note: An example for calibration data and fitted curve can be seen in Schlafer *et al.*, 2015<sup>11</sup>.

### Representative Results

The presented method allows monitoring extracellular pH drops in different microenvironments of dental biofilms in the pH range from 4.5 to 7 in real-time. If the experimental conditions are chosen as described above, pH starts to drop in all areas of the biofilms shortly after exposure to glucose.

When pH in a biofilm drops, bacterial cells become visible within short time (<1 min), as the ratiometric dye is upconcentrated in the cells (**Figure 2A**). In the very beginning, before acid production in the biofilm starts, no difference can be seen between background and cells. Images exported into the software daime have to be segmented with individually chosen brightness thresholds in order to obtain a good congruence between the bacterial biomass in the images and the objects recognized by the program (**Figure 2B**). If segmented appropriately, deletion of objects in daime removes all fluorescent signals that derive from bacterial cells (**Figure 2C**). Subsequent image processing in ImageJ results in green/red ratios for pixels in the extracellular space of the images. With the help of the calibration curve, these ratios can be converted to pH values and visualized with false coloring for graphic representation (**Figure 2D**). Average pH can be calculated for each of the processed images, and the pH development can be followed over time (**Figure 2E**). pH drops may differ between different microscopic fields of view, and both horizontal and vertical pH gradients can be monitored. However, under static conditions, within thin biofilms, only minor vertical pH gradients can be observed.

In some instances, the entire microscopic field of view might be covered with bacterial cells which renders calculation of extracellular pH impossible (**Figure 3A**). The problem might be resolved by choosing a slightly different focus plane. Care must be taken not to overexpose the microscopic images, because the bacterial biomass in the images then covers a larger area than in reality (**Figure 3B**). When segmenting the image in daime it is crucial to choose brightness thresholds that recognize all bacterial cells and, if present, human epithelial cells (**Figure 3C**) as objects. If segmentation is carried out with too high brightness thresholds, intracellular areas will be included in the pH calculation and lead to erroneous results (**Figure 3D**). Monitoring of extracellular pH with the ratiometric dye is limited by the use of confocal microscopy. Up to a penetration depth of 75  $\mu\text{m}$ , extra- and intracellular areas can be distinguished reliably (**Figure 3E**). To measure vertical pH gradients in thicker biofilms, microelectrodes remain the method of choice.



**Figure 1: Acrylic Splint for Intraoral Biofilm Collection.** The splint is designed with buccal acrylic flanges connected by a lingual orthodontic wire that allows the volunteer to bite into normal occlusion. [Please click here to view a larger version of this figure.](#)

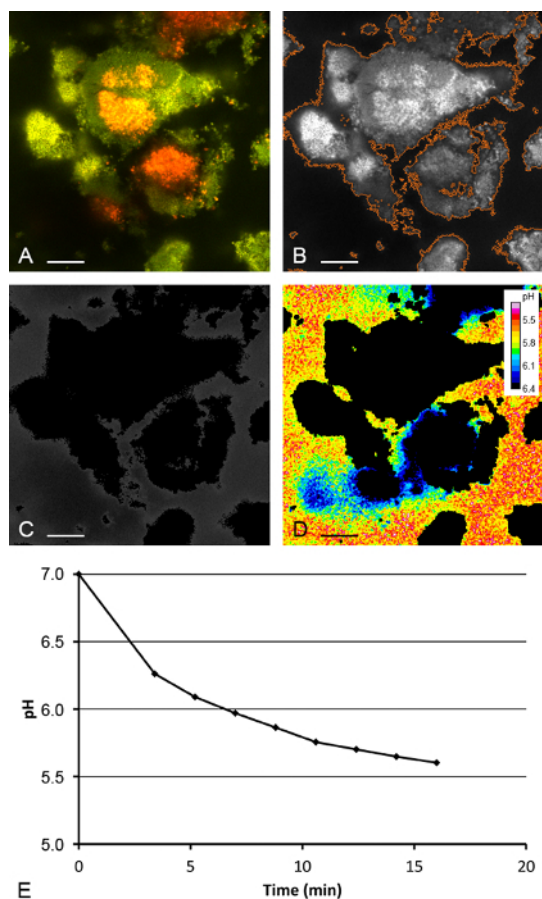


**Figure 2: Image Processing for Microscopic Measurement of Extracellular Biofilm pH.** (A) Confocal microscopic image of a biofilm stained with the ratiometric dye, 9 min after exposure to glucose. The bacterial biomass in the image can be distinguished from the extracellular background. (B) The same image after segmentation in daime. The entire bacterial biomass in the microscopic field of view has been recognized as objects during segmentation, as indicated by the orange lines. (C) The same image after removal of the bacterial biomass. All fluorescence deriving from bacterial cells has been removed, and only fluorescence deriving from the extracellular matrix is left in the image. (D) Graphic representation of extracellular pH in the same microscopic field of view. Green/red ratios have been calculated in ImageJ, and false coloring was applied for graphic representation of extracellular pH. Average extracellular pH = 5.86. (A-D) Scale bars = 20  $\mu$ m. (E) Average pH drop in the same microscopic field of view, monitored for 15 min. The pH drop in this area of the biofilm is quickest in the beginning, shortly after exposure to glucose. Then it slows down but does not reach a plateau within the observation time. [Please click here to view a larger version of this figure.](#)



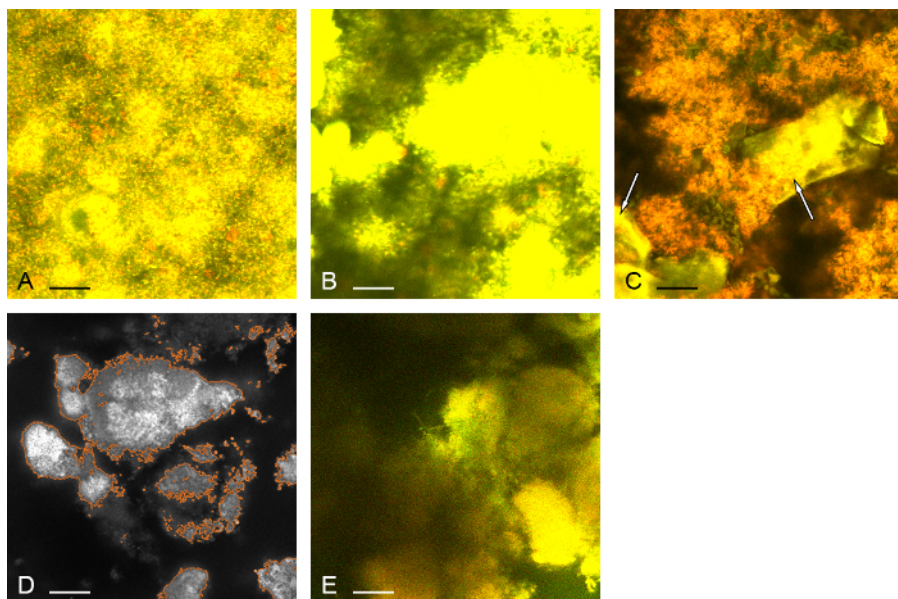


**Figure 3: Microscopic Measurement of Extracellular Biofilm pH - Potential Problems and Mistakes.** (A) Confocal microscopic image of a dense biofilm exposed to glucose and stained with the ratiometric dye. In this microscopic field of view, the entire image is covered with bacterial cells, and removal of the bacteria will not leave extracellular areas for pH calculation. (B) Overexposed confocal microscopic image of a biofilm stained with the ratiometric dye. During image segmentation of overexposed images larger areas than actually covered by bacteria are recognized as objects and part of the extracellular space is lost for pH calculation. (C) Biofilm image with epithelial cells (arrows). Brightness thresholds for image segmentation must be chosen, so that epithelial cells are recognized as objects and removed from the images prior to pH calculation. (D) The same biofilm image as in **Figure 1B**, segmented with a wrong brightness threshold. Part of the bacterial biomass is not recognized as objects and cannot be removed from the image. This leads to inclusion of intracellular areas in the pH calculation and consequently erroneous results. (E) Deep layer of a biofilm stained with the ratiometric dye. The image was acquired 90  $\mu\text{m}$  from the biofilm-substratum interface. Differentiation between extra- and intracellular areas is compromised. Scale bars = 20  $\mu\text{m}$ . [Please click here to view a larger version of this figure.](#)

## Discussion

Microscopic monitoring of biofilm pH provides several advantages, as compared to electrode or microelectrode measurements<sup>4-6</sup>. Microscopic techniques permit to determine pH with a high spatial resolution and allow capturing both horizontal and vertical pH gradients in biofilms without disturbing the biofilm mechanically. Previous attempts of microscopic pH monitoring, however, failed to differentiate between extracellular and intracellular pH in the biofilms<sup>1,7,9</sup>. Due to bacterial homeostasis, intracellular pH differs from extracellular pH, and pH calculations cannot be valid if both intra- and extracellular compartments contribute to the recorded fluorescent emission. The use of a second fluorescent dye along with the pH sensitive dye to visualize bacterial cells is problematic, since even a small overlap between the emission spectra of the dyes might compromise the quantification of fluorescent light. Therefore the technique presented here relies on a concentration gradient of the ratiometric dye between extra- and intracellular compartments of the biofilm to identify and later remove bacterial cells from the acquired pH images.

Upon staining with the fluorescent dye, bacterial cells in biofilms internalize and up-concentrate the molecule, but only in acidic conditions. pH ratiometry with the dye is therefore limited to the pH range between 4.5 and 7.0. At pH values above 7, the unprotonated and thus charged dye does not penetrate bacterial cells well enough to distinguish them from the extracellular background, and at pH values below 4.5 most of the dye molecules are protonated and no further changes in the fluorescent emission can be observed. The fitted curve (pH vs. Ratio green/red) is steepest around pH 6 and flattens out towards pH 4.5. An example is shown in Schlafer *et al.*, 2015, Figure S2.<sup>11</sup> At present the use of the fluorescent dye for pH ratiometry is limited to monitoring extracellular pH<sup>1</sup>. In principle, the dye might also be used to monitor intracellular bacterial pH changes, but so far, calibration has not been performed for intracellular use. Additionally, it would be difficult to distinguish accurately between intracellular fluorescent emission and fluorescent light deriving from dye molecules attached to the outside of the bacterial cell wall. Moreover, as staining with the ratiometric dye is used in combination with confocal microscopy, image acquisition in biofilm layers deeper than 75  $\mu\text{m}$  from the cover glass/biofilm interface is compromised. Decreasing contrast between bacterial cells and extracellular matrix renders the differentiation between intra- and extracellular areas difficult. The employed ratiometric dye has been shown to reliably visualize 15 bacterial species associated with dental biofilm, and it stains all bacterial cells in dental biofilms grown *in situ*<sup>11</sup>. While it is likely that the ratiometric dye is a universal bacterial stain, this has not yet been proven and the stain needs to be tested on biofilms from other habitats than the oral cavity. The method does not permit to produce technical replicates of a given pH measurement, as image acquisition takes some seconds and biofilm pH changes dynamically. Repeated imaging of biofilm-free buffer solutions, however, and repeated imaging of biofilms in buffer yielded stable pH values (data not shown).

All steps of the above described procedure for image processing must be followed accurately. Biofilm images must be acquired with sufficient laser power/gain to obtain adequate levels of fluorescent signal in the extracellular matrix, but overexposure of bacterial cells should be avoided. If bacterial cells are overexposed (too high laser power or gain) larger areas than actually covered by bacteria are recognized as objects during image segmentation and part of the extracellular space is lost for pH calculation (see **Figure 3B**). On the other hand, if images are acquired with very low laser power/gain, fluorescent intensity in the extracellular space might not be sufficient for reliable calculation of green/red emission ratios. A Range Indicator tool in the microscope software might be used to adjust the microscope settings, so that bacterial cells are captured

with maximum intensity, but without overexposure. Automated image segmentation must be controlled for all biofilm images to assure that all bacterial and, if present, eukaryotic cells are recognized as objects by the software. After segmentation, all biofilm images should be compared one by one to the respective unsegmented images to ascertain congruence between the bacterial biomass and the area recognized as objects. If larger areas than those covered by bacteria are recognized as objects the brightness threshold is too low for an accurate differentiation, and segmentation must be performed with a higher brightness threshold. If part of the bacterial biomass is not among the objects, the brightness threshold must be lowered to yield a correct differentiation between extracellular and intracellular space. For the analysis of large datasets it has proven advantageous to segment all images with a row of different brightness thresholds and to subsequently determine the ideal threshold for each image. Once a correct distinction between bacteria and extracellular matrix is achieved, no further problems are to be expected during image processing. There may, however, be some images with a very dense biofilm, where bacteria cover the entire microscopic field of view. In these images, obviously, extracellular pH cannot be determined. In some cases the problem can be resolved by acquiring images in a slightly different z-plane, where the bacterial biomass does not cover the entire field of view.

Further applications of extracellular pH ratiometry might be to study pH landscapes in other microbial communities than dental biofilms (*i.e.* *Pseudomonas aeruginosa* biofilms or current-producing bacterial biofilms). The effect of different ecological parameters, such as oxygen concentration, carbohydrate supply or application of electric current on biofilm pH might be determined. The influence of biofilm age, biofilm thickness and metabolic activity on pH might be investigated, as well as the effect of pH modulating agents on bacterial biofilms. The latter is particularly relevant in the context of dental biofilms, where buffering agents represent a promising therapeutic approach to control dental caries<sup>15</sup>. Moreover, future research should focus on applying the presented method under flow conditions. To date extracellular pH ratiometry has only been used to monitor pH under static conditions. Constant supply of fresh oxygenated medium is likely to have a considerable impact on the development of pH microenvironments and, in particular, vertical pH gradients within thin biofilms. The clearance of acids by medium flow might contribute to the establishment of vertical gradients even in very thin biofilms.

Ratiometric confocal microscopic imaging with the ratiometric dye C-SNARF-4 in combination with precise postprocessing of the acquired digital images permits to calculate and visualize biofilm pH in the extracellular matrix, in real time, in the pH range between 4.5 and 7.0 and up to a biofilm thickness of 75  $\mu\text{m}$ .

## Disclosures

The authors have nothing to disclose.

## Acknowledgements

The authors would like to thank Javier E. Garcia and Lene Grønkjær for technical assistance and Merete K. Raarup for fruitful discussions. This work was funded by Aarhus University Research Foundation and the Simon Spies Foundation.

## References

- Hunter, R.C., & Beveridge, T.J. Application of a pH-sensitive fluoroprobe (C-SNARF-4) for pH microenvironment analysis in *Pseudomonas aeruginosa* biofilms. *Appl. Environ. Microbiol.* **71** (5), 2501-2510 (2005).
- Takahashi, N., & Nyvad, B. Caries ecology revisited: microbial dynamics and the caries process. *Caries Res.* **42** (6), 409-418 (2008).
- Schlafer, S. *et al.* pH landscapes in a novel five-species model of early dental biofilm. *PLoS One.* **6** (9), e25299 (2011).
- von Ohle, C., *et al.* Real-time microsensor measurement of local metabolic activities in ex vivo dental biofilms exposed to sucrose and treated with chlorhexidine. *Appl. Environ. Microbiol.* **76** (7), 2326-2334 (2010).
- Revsbech, N.P. Analysis of microbial communities with electrochemical microsensors and microscale biosensors. *Methods Enzymol.* **397**, 147-166 (2005).
- Vanhoudt, P., Lewandowski, Z., & Little, B. Iridium oxide pH microelectrode. *Biotechnol. Bioeng.* **40** (5), 601-608 (1992).
- Franks, A.E. *et al.* Novel strategy for three-dimensional real-time imaging of microbial fuel cell communities: monitoring the inhibitory effects of proton accumulation within the anode biofilm. *Energy & Environmental Science.* **2** (1), 113-119 (2009).
- Hidalgo, G. *et al.* Functional tomographic fluorescence imaging of pH microenvironments in microbial biofilms by use of silica nanoparticle sensors. *Appl. Environ. Microbiol.* **75** (23), 7426-7435 (2009).
- Vroom, J.M. *et al.* Depth penetration and detection of pH gradients in biofilms by two-photon excitation microscopy. *Appl. Environ. Microbiol.* **65** (8), 3502-3511, (1999).
- Bender, G.R., Sutton, S.V., & Marquis, R.E. Acid tolerance, proton permeabilities, and membrane ATPases of oral streptococci. *Infect. Immun.* **53** (2), 331-338, (1986).
- Schlafer, S. *et al.* Ratiometric imaging of extracellular pH in bacterial biofilms using C-SNARF-4. *Appl. Environ. Microbiol.* **81**(4):1267-73 (2015).
- Dige, I., Nilsson, H., Kilian, M., & Nyvad, B. In situ identification of streptococci and other bacteria in initial dental biofilm by confocal laser scanning microscopy and fluorescence in situ hybridization. *Eur. J Oral Sci.* **115** (6), 459-467 (2007).
- de Jong, M.H., van der Hoeven, J.S., van OS, J.H., & Olijve, J.H. Growth of oral *Streptococcus* species and *Actinomyces viscosus* in human saliva. *Appl. Environ. Microbiol.* **47** (5), 901-904, (1984).
- Daims, H., Lucker, S., & Wagner, M. daime, a novel image analysis program for microbial ecology and biofilm research. *Environ. Microbiol.* **8** (2), 200-213 (2006).
- Liu, Y.L., Nascimento, M., & Burne, R.A. Progress toward understanding the contribution of alkali generation in dental biofilms to inhibition of dental caries. *Int. J Oral Sci.* **4** (3), 135-140 (2012).